ELSEVIER

Fusion Engineering and Design 27 (1995) 515–521

Fusion Engineering and Design

Fatigue life of the plasma-facing components in PULSAR

Jeffrey A. Crowell, James P. Blanchard and the PULSAR Team

Fusion Technology Institute, University of Wisconsin—Madison, 1500 Johnson Drive, Madison, WI 53706-1687, USA

Abstract

The PULSAR project is a multi-institutional effort to determine the advantages that can be gained by building a tokamak with an entirely inductive current drive. This machine, which would operate in a pulsed mode, would feature reduced capital and operating costs compared with steady-state devices requiring complex current drive systems. However, a pulsed reactor would need an energy storage system and face greater structural demands from cyclic fatigue. This paper presents the results of the fatigue analyses for the plasma-facing components of PULSAR. PULSAR features two major engineering designs: a liquid lithium-cooled vanadium alloy design and a helium-cooled silicon carbide composite design. Results are given for each. It is shown that the superior thermal and strength properties of the vanadium alloy allow a much wider spectrum of design options. The SiC composite properties cause significantly more difficulty for the designer and, in particular, no credible design is found for a divertor fabricated solely from the SiC composite. This conclusion is based on current (limited) data for the thermophysical properties and fatigue strength of SiC fiber composites. The developments in these composites needed to create a viable SiC composite diverter are discussed.

1. Introduction

Since the STARFIRE study, most tokamak reactor studies have been conducted under the assumption that non-inductive current drive was necessary for the reactor to be economically feasible. Unfortunately, the non-inductive current drives have proven to be extremely expensive (owing to their relative inefficiency and elaborate hardware), perhaps exceeding the costs incurred by designing for the pulsed operation of an inductively driven machine. The PULSAR study was initiated to investigate this trade-off.

The pulsed nature of PULSAR introduces several design issues that are not present in steady-state devices. These issues include fatigue in the poloidal and toroidal field magnets, fatigue in any pumps and valves that must be cycled during each reactor pulse, thermal cycling of any component which undergoes temperature transients during each pulse, and fatigue in components which experience pressure fluctuations. The magnet fatigue, identified as a critical issue during this study, is dealt with elsewhere. With respect to the pumps and valves, a portion of the shield has been used to store heat between power cycles, thus minimizing the number of components which must undergo thermal and pressure cycles. This paper addresses the key remaining issue: thermal fatigue in the plasma-facing components (first wall and divertor).

There are two PULSAR engineering designs. PULSAR-I is a helium-cooled reactor built from SiC/SiC composite structural materials, while PULSAR-II is a lithium-cooled reactor built from a vanadium alloy

0920-3796/95/$09.50
SSDI 0920-3796(94)00102-2

structural material. In each of these designs, high-cycle fatigue is an important consideration for the 40 000 cycle life desired for each design and must be considered in the thermostructural design of the plasma-facing components. Fatigue data are sparse for these materials, but in each case data have been found for similar materials in order to assess the potential of these materials to withstand the loads expected in PULSAR, as well as to estimate the penalties that must be paid for using a pulsed device.

2. Methodology

2.1. Failure criteria

Both the stress limits imposed by fatigue considerations and the allowable static stresses used in this study follow the guidelines of the ASME Boiler and Pressure Vessel Code [1]. For fatigue, the Code recommends a safety factor of two in the design stress or 20 in the number of cycles, whichever gives the lower design stress. In all cases considered for PULSAR, the safety factor of two on stress is the limiting case. The peak primary stresses (due to the coolant pressure) are limited to the allowable stress intensity S_{mt}. For the vanadium alloy design, the peak secondary stresses (thermal + pressure stresses) are limited to $3S_{mt}$, although fatigue restrictions superseded this limit under all the conditions that were studied. Criteria for choosing secondary stress limits in the SiC composite are not well defined. The ARIES-I study [2] chose two-thirds of the longitudinal ultimate strength as a limit for the combined primary and secondary stress based on thermal-shock testing of this material; we adopt that limit here.

Off-normal loads were not considered in this study. In particular, disruptions have not been accounted for in the analysis.

Radiation damage in the form of swelling, transmutation, etc. limit both the first wall and divertor to 7.5 and 8.4 full power years for the SiC composite and vanadium alloy designs respectively. We anticipate a 7400 s cycle (7200 s burn time and 200 s dwell time), thus the first wall and divertor would undergo 32 000 (SiC) and 36 000 (V) cycles in this time. For this study, we used 40 000 cycles as the goal for both designs.

2.2. Vanadium alloy properties

The thermal and mechanical properties of several vanadium alloys have been examined in previous studies [3–7]. Certain alloys have proved resistant to radiation induced swelling and ductility loss and offer low residual activation. Although data on the physical properties of the PULSAR-II reference alloy V–4Cr–4Ti are scarce, the properties of V–15Cr–5Ti are well established and should be similar. Table 1 lists several of the physical properties of V–15Cr–5Ti. The relatively high thermal conductivity, low thermal expansion coefficient and low modulus make it an excellent candidate for thermal loading applications. Note that although this alloy has a melting temperature of 1890 °C, concerns of irradiation embrittlement restrict us to less than 700 °C.

Fig. 1 illustrates the fatigue properties of unirradiated V–15Cr–5Ti. At 40 000 cycles, the allowable alternating

Table 1
Physical properties of V–15Cr–5Ti and SiC/SiC composite

	V–15Cr–5Ti	SiC composite
Thermal conductivity ($W\,m^{-1}\,K^{-1}$)	26.8 at 400 °C 28.0 at 500 °C 29.5 at 600 °C	17.5
Linear thermal expansion ($10^{-6}\,K^{-1}$)	10.4	4.4
Elastic modulus (GPa)	118	364
Poisson's ratio	0.36	0.16
Allowable stress intensity S_{mt} (MPa)	165 [a]	140 [b]
Maximum allowable temperature (°C)	700 [a]	1100 [b]

[a] Smith et al. [3].
[b] ARIES-I final report [2].

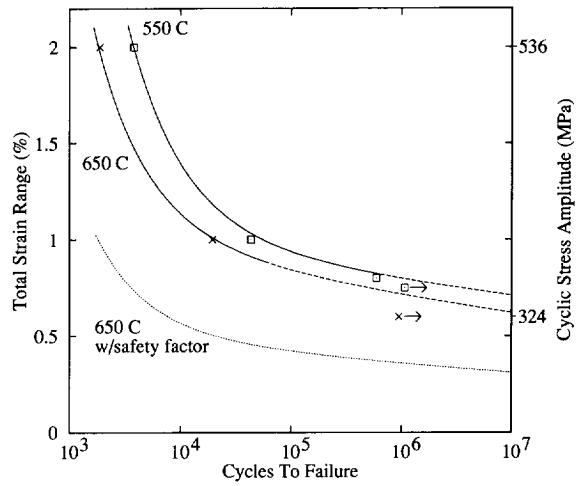

Fig. 1. Fatigue data for unirradiated V–15Cr–5Ti performed in vacuum using fully reversed strain-controlled loading [8].

stress (the alternating stress is half the stress range) is 250 MPa. This is comparable with 316 stainless steel.

2.3. SiC/SiC composite properties

Silicon carbide composites are attractive as structural materials in fusion environments because of their low activation, and high operating temperature and strength. However, at present they lack the fracture toughness of metals and thus are relatively vulnerable to cyclic loads.

The physical properties of composites are generally anisotropic. The ARIES study [2] calculated several material properties of a two-dimensional SiC/SiC composite, using the CLASS code [9] to convert the layer properties and configurations into equivalent orthotropic properties. These computations yielded nearly isotropic properties; thus in this study we assumed an isotropic material. The values used are shown in Table 1. Note that SiC composites have an unusually high modulus which is detrimental to withstanding thermal loads, but a low thermal expansion coefficient that somewhat compensates.

At present, no SiC/SiC fatigue data are available. However, Holmes [10] performed fatigue tests on unirradiated SiC fiber/Si_3N_4 matrix composites. His results should be indicative of the SiC/SiC fatigue strength and are used here to estimate the impact of high-cycle fatigue on the design. In Holmes' study, the specimens were subjected to tensile fatigue, that is, their mean stress was greater than their alternating stress. To allow comparison with (fully reversed) vanadium data, we have extrapolated the data points using the Goodman relation (see for instance [11]) to an alternating stress at zero mean with an equivalent fatigue life. These data are shown in Fig. 2. The allowable alternating stress for 40 000 cycle life is 65 MPa. Note this is approximately one-quarter of the value for vanadium alloy.

2.4. Configuration

Fig. 3 illustrates the configuration of the first wall reference designs. Both consist of tube sheets with coolant flowing in the poloidal direction. Immediately behind the first wall is the beryllium multiplier. The inner diameter of the coolant channels is 7.5 mm. The vanadium alloy designs use liquid lithium as a coolant; the SiC composite design uses helium. Note that the SiC composite design includes a sacrificial carbon vapor deposited (CVD) SiC layer to extend the first wall life against erosion.

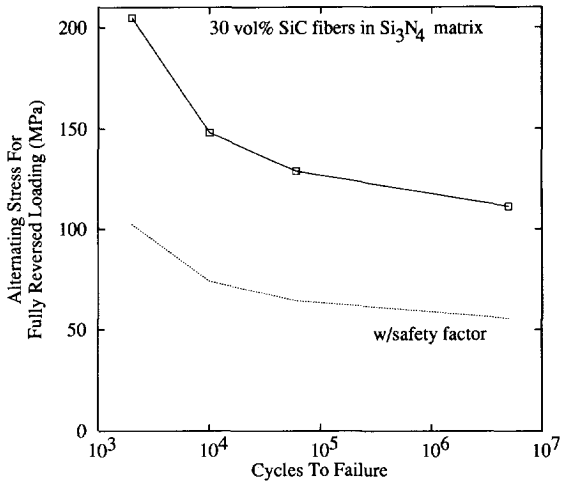

Fig. 2. Fatigue data for SiC/Si_3N_4 composite calculated from tests at non-zero mean stress by the Goodman relation. Experiments were in air at 1200 °C [10].

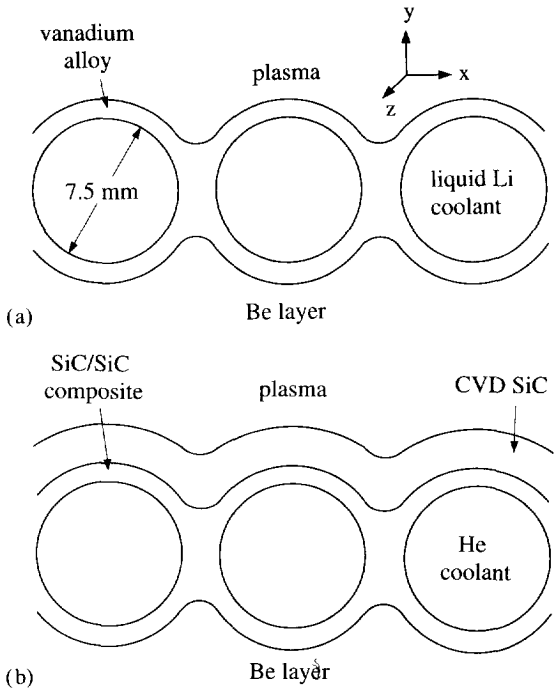

Fig. 3. First wall reference design for PULSAR: (a) vanadium alloy, (b) SiC composite.

The PULSAR divertor designs are similar to the first wall configurations. The vanadium divertor has a larger innner diameter (10 mm). The SiC divertor is made of free-standing tubes with an inner diameter of 5 mm. In

addition, the sacrificial layer is absent from the SiC divertor design.

2.5. Boundary conditions

The manner in which the first wall and divertor are supported has a significant influence on their thermal stresses and thus fatigue life. The tubes must connect to headers at either end of the tube sheet, the weight of the wall must be supported, and the wall must be secured to withstand disruption loads. Thus, to some extent, expansion and bending of the components will be resisted. If expansion is constrained, very large stresses result. Thus, we have presumed that the design permits free expansion. This should not be an unrealistic requirement for the weight and disruption load supports, although it will make the design of the headers difficult.

If the tube sheets of Fig. 3 are unconstrained (simply supported), one-sided heating (from the plasma) will cause them to bend about the x and z-axes. The design details of the structural supports will strongly influence the constraint on this bending and the resulting stress in the material. However, we can bound the stresses by considering two extreme cases: fully constrained ("no") bending and unconstrained ("free") bending. The no-bending boundary condition produces the highest stresses. The plasma-facing surface of each tube is placed in biaxial compression and the blanket-facing surface is placed in biaxial tension. Because the temperature does not vary linearly through the wall, even free-bending induces thermal stresses in the material. They are the lowest stresses attainable for this design.

If we assume continuous tube sheets run the full height of the reactor wall, then supports must be placed periodically along the tubes to control disruption-induced stresses. Thus, bending of the first wall about the x-axis of Fig. 3 will not be possible. This suggests another boundary condition which permits free-bending about the z-axis and no-bending about the x-axis. This "mixed" bending condition will provide a lower bound on the stresses in the first wall because of resistance to bending about the z-axis. Note that mixed-bending generates stresses intermediate to no-bending and free-bending results. Thus, for the first wall, the stresses are bound by no-bending and mixed-bending results.

As a practical matter, the no-bending and mixed-bending results do not differ greatly because the out-of-plane component of the thermal stresses exceeds the in-plane stresses. (Note the large moment of inertia about the x-axis as compared with that about the z-axis.)

2.6. Stress analysis

The stresses in the plasma-facing components of PULSAR were evaluated by the ANSYS finite element code. The use of three-dimensional elements was ruled out owing to their computational burden. However, two-dimensional elements, as given, are unable to simulate the desired boundary conditions because the out-of-plane strains of different elements cannot be coupled to each other. Out-of-plane thermal strains can be calculated once the temperature distribution is known, but to include accurately Poisson effects in the model a different approach is needed. This approach is first to compute the model with no out-of-plane strains. Then use the resulting temperature and two-dimensional stress distribution to determine the out-of-plane strains. Finally, apply loads to the model so as to simulate the out-of-plane strains. If accurate Poisson effects are important, they can be determined by iterating this procedure.

2.7. Loads

Table 2 shows the peak radiative and neutron heating loads that the plasma-facing components are expected to absorb. In addition, the beryllium multiplier conducts part of its internally generated heat to the blanket-facing side of the first wall, applying a heat flux of 0.135 MW m^{-2} to this surface. The neutron heating in

Table 2
Thermal and mechanical loads and properties of the first wall and divertor designs

	PULSAR-II (V alloy)	PULSAR-I (SiC composite)
First wall heat flux (MW m^{-2})	0.27	0.37
Divertor heat flux (MW m^{-2})	4.1	3.3
Neutron heating (MW m^{-3})	8.4	6.3
Coolant pressure (MPa)	2	10
First wall heat transfer coefficient (W m^{-2} K^{-1})	10 000	3153
Divertor heat transfer coefficient (W m^{-2} K^{-1})	34 700	15 600

the first wall was found to have a negligible effect in comparison with the radiative heat load. Note that the SiC composite design must tolerate a coolant pressure five times higher than the vanadium design.

3. First wall results

Fig. 4 shows the results of the first wall fatigue analysis in terms of maximum permissible heat flux as a function of wall thickness. For the vanadium alloy structure (Fig. 4(a)), the maximum wall thickness is in excess of 2 mm which allows erosion rates (presently uncertain) to be more than 240 μm per year. The SiC design does not perform as well as vanadium but is acceptable. Fig. 4(b) shows results for 0.5 mm and 1 mm CVD coating thicknesses. Erosion of SiC must be slower than 130 μm per year for this design (assuming 0.5 mm CVD coating).

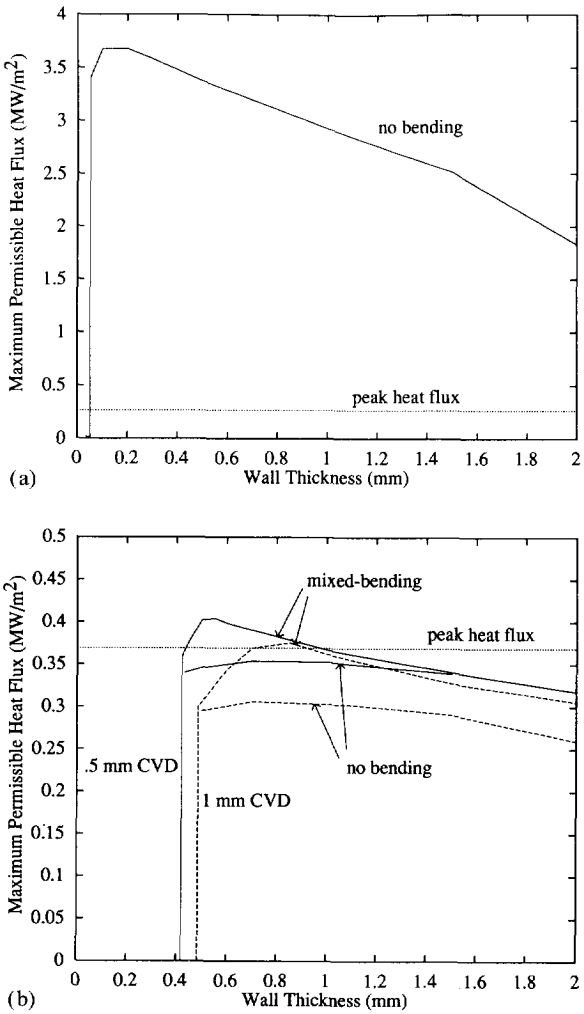

Fig. 4. First wall maximum permissible heat flux vs. wall thickness for (a) vanadium alloy and (b) SiC composite for 0.5 mm and 1 mm thick CVD layers (the wall thickness does not include the CVD layer).

The most damaging stresses for fatigue in the vanadium design were located on the plasma-facing surface. This is a result of the cycling between tensile stress when the plasma is off and large out-of-plane compressive stresses when the plasma is on. By contrast, the highest primary stresses are on the coolant channel surface. The SiC composite first wall had a more complex stress distribution owing to the sacrificial layer. In general, the highest stresses were in the blanket-facing wall.

4. Divertor results

The divertor presented a much more substantial challenge to the materials because the heat fluxes are about an order of magnitude larger. Fortunately, the divertor is a relatively small component compared with the first wall. Higher coolant velocities, internal fins, and other heat transfer enhancements that would require unacceptable pumping power in the first wall were employed here to raise the heat transfer coefficients. Their values are listed in Table 2. Further, much shorter modules might be used so that free-bending conditions could be approached.

However, the vanadium alloy divertor will not require a special tube design. As Fig. 5(a) indicates, wall thicknesses up to 1.4 mm are acceptable under no-bending conditions.

Unfortunately, even with a five-fold increase in heat transfer coefficient (3000 to 15 000 $W\,m^{-2}\,K^{-1}$) and completely unconstraining supports, the SiC composite design fails to tolerate the divertor's heat flux at any wall thickness, see Fig. 5(b). For free-bending boundary conditions, the curve reaches a maximum at 2.75 $MW\,m^{-2}$. An improvement of 19% in the permissible heat flux is needed (in addition to some kind of erosion protection).

The largest thermal stresses in the divertor are a strong function of both the heat transfer coefficient to the coolant and the thermal conductivity. As these parameters are increased, the maximum stresses are

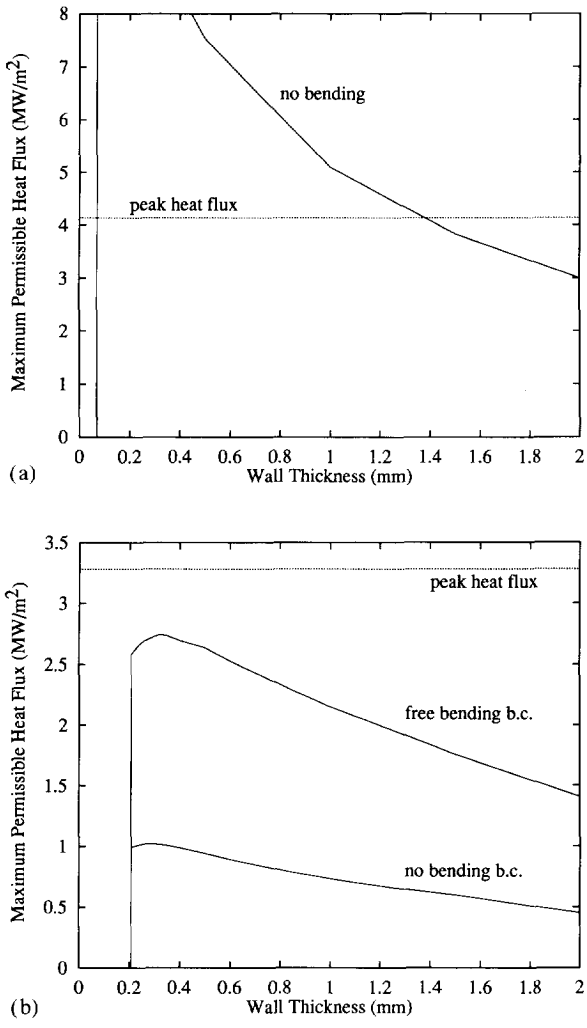

Fig. 5. Divertor maximum permissible heat flux vs. wall thickness for (a) vanadium alloy and (b) SiC composite.

reduced. Fig. 6 illustrates the increases in these parameters needed to make a viable divertor (assuming a 1 mm thick tube wall). The analysis shows that further improvements in the heat transfer coefficient will not improve the design unless the thermal conductivity can also be increased. In fact, the thermal conductivity must be at least 25 $W m^{-1} K^{-1}$ for a free-bending design to become acceptable. As Fig. 6 shows, a design constrained from bending would require drastic improvements in these parameters; for a successful SiC composite divertor, short tube lengths and compliant headers are imperative.

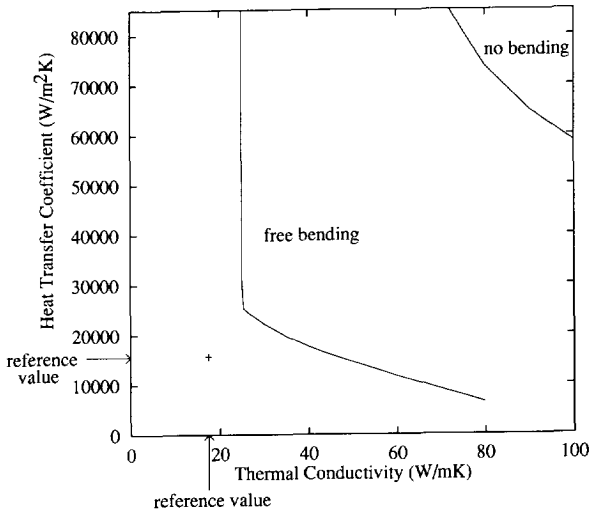

Fig. 6. Minimum heat transfer coefficient and thermal conductivity required for a viable SiC composite divertor under free- and no-bending conditions (that is, with very compliant and very rigid supports).

5. Conclusions

Our investigation found that both PULSAR first wall designs were acceptable provided erosion rates are limited to 240 μm per year for the vanadium alloy design and 130 μm per year for the SiC composite design. The vanadium divertor was also acceptable, though erosion must be less than 160 μm per year if the divertor is to last 40 000 cycles. The SiC composite divertor is not acceptable. Design of a viable SiC composite divertor will require a thermal conductivity greater than 25 $W m^{-1} K^{-1}$, still greater improvements in the heat transfer coefficient, tubes short enough and headers compliant enough to approach free-bending conditions and very low erosion rates.

Acknowledgements

Support for this work has been provided by the United States Department of Energy under contract number DE-FG02-89ER52158.

References

[1] ASME Boiler and Pressure Vessel Code, ASME, 1989, Sec. III, Div. 1, App. III, pp. 268–270.

[2] ARIES-I Tokamak Reactor Study, Final Report, UCLA-PPG-1323 (University of California, Los Angeles, CA), pp. 8-33–8-35.
[3] D.L. Smith et al., Blanket Comparison and Selection Study, Final Report, ANL/FPP-84-1, 1984 (Argonne National Laboratory).
[4] D.L. Smith, B.A. Loomis and D.R. Diercks, Vanadium-base alloys for fusion reactor applications—a review, J. Nucl. Mater., 135 (1985) 125–139.
[5] D.N. Braski, The effect of neutron irradiation on vanadium alloys, J. Nucl. Mater., 141–143 (1986) 1125–1131.
[6] M.L. Grossbeck and J.A. Horak, Tensile properties of V–15Cr–5Ti following neutron irradiation and helium implantation, Radiat. Effects, 101 (1986) 169–171.
[7] J.W. Davis, T.A. Lechtenberg, D.L. Smith and F.W. Wiffen, Structural materials data base assessment for the blanket comparison and selection study, Fusion Technol., 8 (1985) 1927–1943.
[8] K.C. Liu, High temperature fatigue behavior of unirradiated V–15Cr–5Ti tested in vacuum, J. Nucl. Mater., 103–104 (1981) 913–918.
[9] J.J. Kibler, Composite Laminate Analysis System (CLASS), Materials Science Corp., ASM International, Metals Part, OH, 1987.
[10] J.W. Holmes, Influence of stress ratio on the elevated-temperature fatigue of a silicon carbide fiber-reinforced silicon nitride composite, J. Am. Ceram. Soc., 74(7) (1991) 1639–1645.
[11] R.C. Juvinall, Fundamentals of Machine Component Design, Wiley, New York, 1983, pp. 216–220.